2026, 66(3): 1294-1310
CSTR: 32112.14.j.AMS.20250785
DOI: 10.13343/j.cnki.wsxb.20250785

微生物学报
Acta Microbiologica Sinica
http://journals.im.ac.cn/actamicrocn

Research Article 研究报告

娄彻氏链霉菌 D74 菌丝多糖促进丹参毛状根生长和丹参酮积累

马芳[1,2#]，张冰颖[1#]，李洋[1]，王思雨[1]，薛泉宏[3]，杜宏涛[1,2*]，阎岩[1*]

1 延安大学 生命科学学院，陕西省黄土高原资源植物研究与利用重点实验室，陕西 延安
2 延安大学 生命科学学院，微生物资源开发与绿色循环利用陕西省高校工程研究中心，陕西 延安
3 西北农林科技大学 资源环境学院，陕西 杨凌

马芳, 张冰颖, 李洋, 王思雨, 薛泉宏, 杜宏涛, 阎岩. 娄彻氏链霉菌 D74 菌丝多糖促进丹参毛状根生长和丹参酮积累[J]. 微生物学报, 2026, 66(3): 1294-1310.

MA Fang, ZHANG Bingying, LI Yang, WANG Siyu, XUE Quanhong, DU Hongtao, YAN Yan. Mycelial polysaccharide from *Streptomyces rochei* D74 promotes growth and tanshinone accumulation of *Salvia miltiorrhiza* hairy roots[J]. Acta Microbiologica Sinica, 2026, 66(3): 1294-1310.

摘　要：【目的】以娄彻氏链霉菌(*Streptomyces rochei*) D74 为材料，系统分离纯化其菌丝体多糖(*Streptomyces rochei* polysaccharide, SRP)，解析其精细结构，并评价纯化多糖组分对丹参毛状根生长及丹参酮生物合成的影响及其作用机制。【方法】采用热水浸提法提取粗多糖，经乙醇沉淀、Sevag 法脱蛋白后依次通过 DEAE-52 阴离子交换柱与 Sephadex G-100 凝胶柱进行纯化。运用傅里叶变换红外光谱 (Fourier transform infrared spectroscopy, FT-IR)、高效液相色谱-质谱联用(high performance liquid chromatography-mass spectrometry, HPLC-MS) 及核磁共振(nuclear magnetic resonance, NMR)等技术对主要活性组分 SRP-W-2 的理化性质及结构进行系统表征。进一步通过测定丹参毛状根生物量、丹参酮含量及关键合成基因表达水平，评估 SRP-W-2 对毛状根生长与丹参酮合成的调控作用。【结果】SRP-W-2 的得率为 2.41%，主要由葡萄糖与半乳糖组成(物质的量比为 12.53:1)。结构解析表明，SRP-W-2 的主链由→4)-α-D-Glc*p*-(1→和→4)-α-D-Gal*p*-(1→单元构成，分支点位于→4,6)-α-D-Glc*p*-(1→和→4,6)-α-D-Gal*p*-(1→，分支结构为 α-D-Glc*p*-(1→4)-α-D-Glc*p*-(1→。生物活性实验显示，SRP-W-2 可显著促进丹参毛状根生物量与丹参酮类成分的积累。在 50 mg/L SRP-W-2 处理 15 d 后，毛状根干重提升 37.52%；隐丹参酮 (cryptotanshinone, CT)、二

资助项目：国家自然科学基金(21602178)；延安大学博士科研启动项目(205040406, 205040422)；延安大学大学生创新创业训练计划(D2024158)

This work was supported by the National Natural Science Foundation of China (21602178), the Doctoral Research Initiation Project of Yan'an University (205040406, 205040422), and the Innovation Training Program for College Students of Yan'an University (D2024158).

#These authors contributed equally to this work.
*Corresponding authors. E-mail: DU Hongtao, duhongtao8410@163.com; YAN Yan, yanyan081124@163.com

Received: 2025-10-20; Accepted: 2025-11-27; Published online: 2025-12-08

氢丹参酮 I (dihydrotanshinone I, DT-I)、丹参酮 I (tanshinone I, T-I)和丹参酮 IIA (tanshinone IIA, T-IIA)含量分别提高至对照组的 19.0 倍、6.4 倍、2.8 倍和 4.8 倍。基因表达分析进一步表明，SRP-W-2 可上调丹参酮合成途径关键基因 *HMGR*、*DXS*、*DX*R 和 *GGPPS* 的表达。【结论】娄彻氏链霉菌 D74 来源的多糖组分 SRP-W-2 可同步促进丹参毛状根的生长与丹参酮的生物合成，具备作为高效诱导剂的潜力，为丹参资源的开发提供了新策略。

关键词：娄彻氏链霉菌 D74；菌丝多糖；丹参毛状根；丹参酮

Mycelial polysaccharide from *Streptomyces rochei* D74 promotes growth and tanshinone accumulation of *Salvia miltiorrhiza* hairy roots

MA Fang[1,2#], ZHANG Bingying[1#], LI Yang[1], WANG Siyu[1], XUE Quanhong[3], DU Hongtao[1,2*], YAN Yan[1*]

1 Shaanxi Key Laboratory of Research and Utilization of Resource Plants on the Loess Plateau, College of Life Sciences, Yan'an University, Yan'an, Shaanxi, China

2 Engineering Research Center of Microbial Resources Development and Green Recycling, University of Shaanxi Province, College of Life Sciences, Yan'an University, Yan'an, Shaanxi, China

3 College of Natural Resources and Environment, Northwest A&F University, Yangling, Shaanxi, China

Abstract: [Objective] To systematically isolate and purify the polysaccharide from the mycelium of *Streptomyces rochei* D74 (SRP), elucidate its fine structure, and evaluate the effect of the purified polysaccharide fraction on the growth of *Salvia miltiorrhiza* hairy roots and the biosynthesis of tanshinones, along with the underlying mechanism. **[Methods]** The crude polysaccharide was extracted using hot water, which was followed by ethanol precipitation and deproteinization *via* the Sevag method. Further purification was performed using DEAE-52 anion-exchange chromatography and Sephadex G-100 gel filtration chromatography. The physicochemical properties and structural features of the main active fraction, SRP-W-2, were systematically characterized by Fourier transform infrared spectroscopy (FTIR), high performance liquid chromatography-mass spectrometry (HPLC-MS), and nuclear magnetic resonance (NMR). The effects of SRP-W-2 on hairy root growth and the biosynthesis of tanshinones were assessed by measuring biomass, tanshinone content, and the expression levels of key biosynthetic genes. **[Results]** SRP-W-2 was obtained with a yield of 2.41%. It was primarily composed of glucose and galactose at a molar ratio of 12.53∶1. Structural analysis revealed that the backbone of SRP-W-2 consisted of →4)-α-D-Glc*p*-(1→ and →4)-α-D-Gal*p*-(1→ residues, with branching points at →4,6)-α-D-Glc*p*-(1→ and →4,6)-α-D-Gal*p*-(1→. The side chain was identified as α-D-Glc*p*-(1→4)-α-D-Glc*p*-(1→. Bioactivity assays demonstrated that SRP-W-2 significantly enhanced both the biomass of *S. miltiorrhiza* hairy roots and the accumulation of tanshinones. After 15 d of treatment with 50 mg/L SRP-W-2, the dry weight of the hairy roots increased by 37.52%. Meanwhile, the content

of cryptotanshinone (CT), dihydrotanshinone I (DT-I), tanshinone I (T-I), and tanshinone IIA (T-IIA) was increased by 19.0-fold, 6.4-fold, 2.8-fold, and 4.8-fold, respectively. Gene expression analysis further indicated that SRP-W-2 up-regulated key genes involved in the tanshinone biosynthetic pathway, including *HMGR*, *DXS*, *DXR*, and *GGPPS*. **[Conclusion]** The polysaccharide fraction SRP-W-2 from *S. rochei* D74 simultaneously promoted the growth of *S. miltiorrhiza* hairy roots and the biosynthesis of tanshinones, demonstrating its potential as an effective elicitor. This study provided a new strategy for the utilization and development of *S. miltiorrhiza* resources.

Keywords: *Streptomyces rochei* D74; mycelial polysaccharide; *Salvia miltiorrhiza* hairy roots; tanshinones

Tanshinones are a key group of bioactive diterpenoids found in *Salvia miltiorrhiza* (*S. miltiorrhiza*), a plant widely used in traditional medicine. These compounds exhibit notable pharmacological properties, particularly in the prevention and treatment of cardiovascular diseases[1-3]. Their clinical and commercial significance is highlighted by the widespread use of tanshinone-based formulations such as the Danshen Dripping Pill, which achieves annual sales exceeding $200 million[4-5]. However, the sustainable supply of tanshinones is hampered by two major limitations. First, their natural content in the plant is very low, making extraction inefficient and costly. Second, field-grown *S. miltiorrhiza* is prone to pest and disease damage, often leading to pesticide residues and inconsistent herb quality[6]. To address these challenges, researchers are turning to biotechnological strategies. Methods such as hairy root culture and metabolic engineering are being developed to increase tanshinone production and achieve scalable, controlled manufacturing[7-10].

Hairy roots culture (HRC) induced by *Agrobacterium rhizogenes* is regarded as a highly promising biotechnological strategy for the production of secondary metabolites (SMs) due to its rapid growth rate, cost-effectiveness, independence from seasonal variations, and ability to yield comparable or even higher quantities of valuable SMs compared to normal root cultures[11-12].

The technique has been developed for the production of bioactive compounds in various plants, such as scopolamine, tanshinone, triptolide and (*E*)-β-farnesene[13-15]. Currently, an increasing body of research has demonstrated the utilization of exogenous substances such as biotic elicitors (polysaccharides, chitin, and pectin) and abiotic elicitors (metal nanoparticles, jasmonates, salicylic acid, and gibberellic acid) to stimulate the production of SMs in HRC[16-17]. Although the common elicitors have been shown to enhance tanshinones production of HRC in *S. miltiorrhiza*, it is noteworthy that most of these elicitors exert inhibitory effects on biomass yield of HRC[18-21].

Streptomyces rochei D74 is a kind of actinomycetes which can promote plant growth and inhibit plant pathogens[22-24]. The previous study revealed that the polysaccharide derived from *Streptomyces rochei* D74 exhibited enhanced efficacy in promoting root growth and tanshinones production in HRC of *S. miltiorrhiza*. To further investigate the structure and bioactivity, we isolated and purified a homogeneous neutral polysaccharide named SRP-W-2 in this study. The detailed structure of SRP-W-2 was analyzed and identified through monosaccharide composition analysis, methylation analysis, deacetylation reaction, as well as 1D/2D NMR spectroscopy. Moreover, we examined the effects of SRP-W-2 on roots growth and tanshinones production in *S. miltiorrhiza* HRC. Finally, to elucidate the potential regulatory mechanism, we evaluated the expression of genes encoding key enzymes involved in tanshinone biosynthesis in *S. miltiorrhiza* HRC.

1 Materials and methods

1.1 Materials and chemicals

Streptomyces rochei D74 mycelia was kindly provided by Professor Xue Quanhong from the College of Resources and Environment at Northwest A&F University. Monosaccharide and tanshinones standards, as well as other organic reagents, were purchased from Shanghai Aladdin Biochemical Technology Co., Ltd.. The chemicals used in this study were analytical grade.

1.2 Isolation and purification of the polysaccharide

The *Streptomyces rochei* D74 polysaccharide was prepared following a previously described method[24]. Briefly, the mycelia powder was pretreated with petroleum ether and 80% (*V/V*) ethanol at 80 ℃ for 2 h (repeated twice) to remove pigments, lipids, and some small-molecule materials. Subsequently, the residue was extracted using twice distilled water (*W/V*, 1∶10) in a processor under the following optimized conditions: extraction was performed twice, each for a duration of 2 hours, at a temperature of 90 ℃ . After centrifugation and concentration steps, the supernatant was precipitated with four volumes of anhydrous ethanol and refrigerated overnight at 4 ℃. The precipitate was collected by centrifugation. The Sevag method was used to remove protein and finally the crude polysaccharide (cSRP) was obtained by vacuum freeze-drying.

The cSRP was dissolved in deionized water, followed by filtration through a Millipore filter (0.45 μm). Subsequently, the filtrate was subjected to elution on a DEAE-52 ion exchange cellulose column (2.6 cm×60 cm). After loading, the column was stepwise eluted with aqueous solutions of NaCl at concentrations of 0, 0.2 and 0.5 mol/L, flowing at a rate of 0.8 mL/min. The eluate (5 mL/tube) was automatically collected for subsequent carbohydrate content determination using the phenol-sulfuric acid method at an absorbance wavelength of 490 nm. The initially purified sugar fraction was then freeze-dried and further isolated on a Sephadex G-100 column (1.8 cm×100 cm), employing a flow rate of 0.2 mL/min with deionized water as the eluent. The elution was monitored as described above.

1.3 Characterization of SRP-W-2

1.3.1 Homogeneity and molecular weight determination

The molecular weight of SRP-W-2 was determined using high-performance gel permeation chromatography (HPGPC) on a Waters 600 HPLC System (Waters Corporation), equipped with a 2414 differential refractive index detector. Briefly, three Waters ultrahydrogel columns in series (250, 1 000 and 2 000, dimensions: 30 cm×7.8 mm; particle size: 6 μm) were calibrated using T-series dextran standards with known molecular weights of 5.2, 48.6, and 668 kDa, respectively. The columns were maintained at a constant temperature, and the mobile phase consisted of sodium acetate (3 mmol/L) flowing at a rate of 0.5 mL/min. A sample volume of 50 μL was injected for each run.

1.3.2 Determination of neutral sugar, uronic acid and protein content

The neutral sugar content of SRP-W-2 was determined using the phenol-sulfuric acid method with glucose as a standard[25]. The uronic acid content was assessed through a sulfamate/m-hydroxy-diphenyl assay employing galacturonic acid as a standard[26]. The protein content was quantified following Bradford's method, utilizing bovine serum albumin as the reference standard[27].

1.3.3 Functional group analysis

The functional group analysis of SRP-W-2 was conducted using a Fourier transform infrared (FT-IR) spectrophotometer (Bruker). The dried SRP-W-2 was mixed with spectroscopic grade KBr powder, ground and compressed into a 1 mm pellet for FT-IR spectroscopy in the frequency range of 4 000−450 cm^{-1}.

1.3.4 Monosaccharide composition analysis

The monosaccharide composition of SRP-W-2 was analyzed using the pretreatment method described in our previous study[28]. Briefly, a 200 μL solution of polysaccharide (5 mg/mL) was

subjected to hydrolysis with 200 μL of 2 mol/L trifluoroacetic acid (TFA) in a sealed glass tube at 121 ℃ for 2 hours. After hydrolysis, the solution was evaporated under reduced pressure and the residue was dissolved in 3 mL of methanol before being dried. This process was repeated five times to ensure complete removal of excess TFA. The resulting dried hydrolysate was then dissolved in 400 μL of 0.6 mol/L NaOH and mixed with a solution containing 200 μL of 0.5 mol/L 1-phenyl-3-methyl-5-pyrazolone (PMP) in methanol. The mixture underwent incubation at a temperature of 70 ℃ for a duration of two hours. Subsequently, the reaction solution was neutralized by adding 200 μL of HCl (0.3 mol/L) and extracted three times with chloroform using a volume ratio of aqueous layer to chloroform as approximately equal to one-to-five respectively. Finally, the aqueous layer passed through a nylon membrane filter with pore size set at around 0.45 μm prior to analysis *via* high-performance liquid chromatography (HPLC). The chromatographic conditions employed were as follows: WondaSil C18 column dimensions measuring at 4.6 mm×150 mm with particle size set at around 5 μm from Shimadzu, column temperature maintained at 30 ° C, mobile phase consisting a mixture of phosphate-buffered saline (PBS, 0.1 mol/L, pH 6.7) and acetonitrile in a ratio of 83:17 (*V/V*), flow rate set at 1.0 mL/min, detector wavelength fixed at 245 nm, injection volume standardized as 20 μL.

1.3.5 Glycosyl linkage composition analysis

For glycosyl linkage analysis, SRP-W-2 was subjected to permethylation, depolymerization, reduction, and acetylation. The resulting derivatives were subsequently analyzed using gas chromatography-mass spectrometry (GC-MS), as described by Wang et al[29]. Briefly, 5.0 mg of SRP-W-2 was dissolved in 2 mL of DMSO. After incubating with 10 mg of NaOH powder under nitrogen for 30 min, methyl iodide (250 μL) was added dropwise to the mixture in an ice bath for 1 h. Subsequently, water (5 mL) and chloroform (5 mL) were added, followed by vortexing and centrifugation. The resulting mixture was washed three times with water and the dichloromethane was evaporated. Next, the methylated polysaccharide underwent hydrolysis following the same procedure as described in Section 1.3.4. The resulting hydrolysate was then reduced with 500 μL of 1 mol/L $NaBH_4$ at room temperature for 2 h, and the reaction was terminated by adding acetic acid (100 μL). Acetic anhydride (2 mL) was added to the mixture and thoroughly mixed before being subjected to a reaction at 100 ℃ for 2 h. After allowing it to stand with water (5 mL) for 10 min, dichloromethane (3 mL) was added for extraction of the organic phase which contained acetylated partially methylated alditol acetates that were subsequently analyzed using gas chromatography-mass spectrometry (GC-MS).

1.3.6 Glycosidic linkage sequence analysis

The glycosidic linkage sequence of SRP-W-2 was analyzed by nuclear magnetic resonance (NMR) spectroscopy. The accurately dissolved amount of SRP-W-2, 20.0 mg, was prepared in a dedicated NMR tube containing 0.6 mL of deuterated water (D_2O). Subsequently, the spectra including 1D NMR (^{1}H NMR, ^{13}C NMR) and 2D NMR (^{1}H-^{1}H COSY, HSQC, HMBC) were recorded at 30 ℃ using a high-field 600 MHz NMR instrument (JEOL Resonance Inc.).

1.4 SRP-W-2 treatment of *S. miltiorrhiza* hairy roots

1.4.1 Hairy roots culture

The *S. miltiorrhiza* hairy roots were inoculated with *Agrobacterium rhizogenes* (ATCC 15834), and the stock cultures of the hairy roots were maintained on solid 6,7-V medium at a temperature of 25 ℃ in darkness. In all experiments, 0.3 g of hairy roots (fresh weight) was inoculated into a 100 mL Erlenmeyer flask containing 50 mL of liquid medium and placed on an orbital shaker set at 25 ℃ and 180 r/min. The SRP-W-2 treatment (0, 25, 50 and 100 mg/L) was administered to the culture on day 21 post inoculation. The hairy roots samples were collected at specific time points (0, 5, 10 and 15 days) following the treatment. A

concentration of 50 mg/L *Gracilariopsis lemaneiformis* polysaccharide (GLP) was employed as a parallel control. The roots were filtered, washed three times with distilled water, and oven-dried at 45 °C until reaching a constant dry weight (dw).

1.4.2 HPLC analysis of tanshinones in the *S. miltiorrhiza* roots

The dried hairy roots were finely ground and subjected to ultrasonic extraction with methanol (0.1 g/mL) for 45 minutes. Subsequently, the resulting mixture was centrifuged at a speed of 10 000 r/min for 10 minutes prior to filtration of the supernatant through a 0.45 μm organic membrane filter. Subsequently, the samples were subjected to HPLC analysis using a dedicated program, and the concentrations of CT, DT-I, T-I, and T-IIA were determined employing the internal standard method[30]. The HPLC analysis was performed using an LC-15C system (Shimadzu) equipped with a WondaSil C18 column (4.6 mm× 150 mm, 5 μm, Shimadzu) and UV/Vis detection (Shimadzu).

1.4.3 Detection of key gene expression of tanshinone biosynthesis by real-time quantitative PCR (RT-PCR)

The total RNA of *S. miltiorrhiza* hairy roots was extracted using the Tiangen RNAprep Pure Plant Kit (Tiangen Biotech Co., Ltd.) following the manufacturer's instructions. Subsequently, cDNA synthesis was performed according to the protocol of the PrimeScript™ RT Reagent Kit (TaKaRa). The resulting cDNA served as a template for RT-PCR analysis to evaluate the relative expression of key genes involved in tanshinone biosynthesis. The RT-PCR was conducted following the manufacturer's instructions (TaKaRa), with a pre-denaturation step at 95 ℃ for 30 s followed by denaturation at 95 ℃ for 30 s and annealing at 60 ℃ for 30 s. Fluorescence data were collected from 65 ℃ to 95 ℃ over a span of 40 cycles[30]. All experiments were performed in triplicate. The primer sequences used for RT-qPCR are provided in Table 1

Table 1 The primers of genes used in RT-PCR

Primer names	Primer sequences (5′→3′)
HMGR_F	ACCTCACCAACGGAGTCTTCT
HMGR_R	AGCCGAGGAGATAGATGAAGG
DXR_F	CGCTGGACATAGTTGCTGAA
DXR_R	CAAAATCAGCCAAAGCCTCT
DXS_F	GCGATTCACAGAGAGGTCAAG
DXS_R	GGTTGTGTAAGGCTGAGTTGG
GGPPS_F	TTCAATTTCAACGCCTACGTC
GGPPS_R	GTCGTGGATGAGAGACATGGT
Actin-F	GGTGCCCTGAGGTCCTGTT
Actin-R	AGGAACCACCGATCCAGACA

1.5 Statistical analysis

The data were presented as means±standard deviation (SD). Differences between groups were assessed using Duncan's multiple range tests. A *P*-value<0.05 was considered statistically significant. The graphic presentation in the paper was created using Origin 2021 software.

2 Results and discussion

2.1 Purification and characterization of SRP-W-2

Elucidating the structural features of polysaccharides is critical in glycobiology, given that their diverse bioactivities are determined by aspects such as chemical homogeneity, monomer composition, and structural characteristics. Therefore, we isolated a homogeneous polysaccharide and carried out systematic structural characterization.

2.1.1 Purification analysis

The crude SRP (cSRP, 37.41 g) was extracted from *Streptomyces rochei* D74 mycelia (500 g) using hot water extraction followed by ethanol precipitation (Figure 1A). Subsequently, the cSRP was dissolved in distilled water and fractionated into three fractions (SRP-W, SRP-1, and SRP-2) using a DEAE-52 cellulose column (Figure 1B). Further separation of SRP-W (17.38 g) was achieved through a Sephadex G-100 column, resulting in two fractions: SRP-W-1 (1.15 g) and

SRP-W-2 (12.06 g) (Figure 1C). The predominant fraction (SRP-W-2) was collected for subsequent analysis.

2.1.2 HPGPC analysis

The homogeneity of SRP-W-2 was confirmed by HPGPC analysis. According to the calibration curve, the weight average molecular weight (M_w) and number average molecular weight (M_n) of SRP-W-2 were determined to be 44.7 kDa and 43.8 kDa, respectively. The dispersion coefficient (M_w/M_n) of SRP-W-2 was calculated as 1.02. As depicted in Figure 2A, SRP-W-2 exhibited a single, symmetrical peak, indicating its homogeneous nature as a polysaccharide.

2.1.3 Physical and chemical indicators analysis

The physical and chemical properties of SRP-W-2 were investigated to gather additional information. It was determined that SRP-W-2 is a white powder with solubility in water but

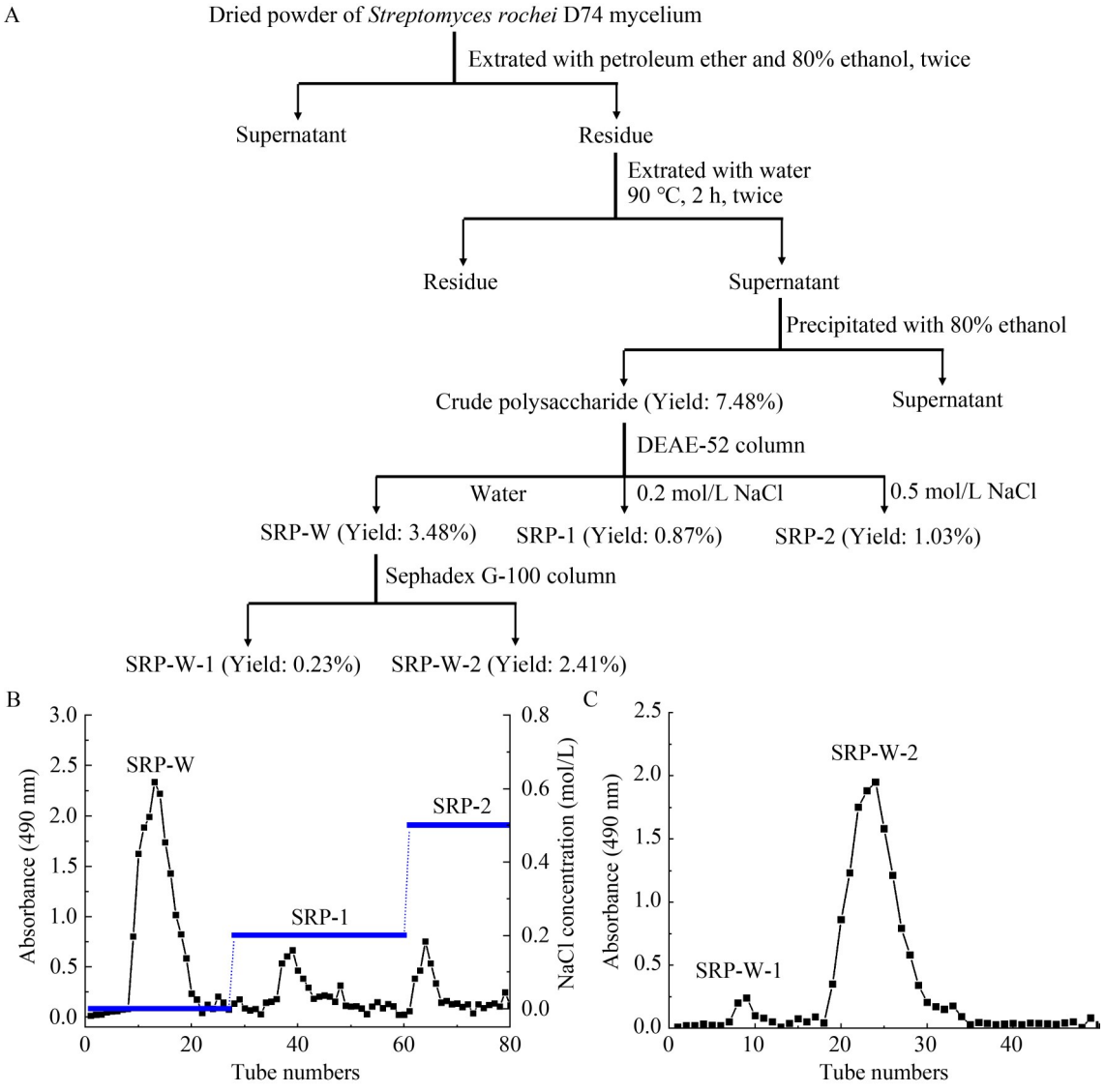

Figure 1 Extraction and purification of the polysaccharide (SRP-W-2). A: The flow chart; B: The elution profile of crude polysaccharide fractions on the DEAE-52 cellulose column; C: The elution curve of SRP-W-2 component on the Sephadex G-100 columns.

insolubility in ethanol and chloroform. The carbohydrate content of SRP-W-2 was found to be 94.82%, while no uronic acid or protein was detected.

2.1.4 FT-IR analysis

The FT-IR spectrum of SRP-W-2 is presented in Figure 2B, exhibiting numerous characteristic absorption peaks associated with polysaccharide. The prominent peaks near 3 406 cm^{-1} and 2 930 cm^{-1} were assigned to O－H stretching vibrations and C－H stretching vibrations, respectively[31]. The weak absorption peak around 1 652 cm^{-1} was attributable to the bound water. The C－H bending vibrations were observed at 1 419 cm^{-1} and 1 364 cm^{-1}. The presence of C−O−C and C−O−H linkages in the pyranose was indicated by three absorption peaks observed at 1 154, 1 080, and 1 023 cm^{-1}. Furthermore, the distinctive absorption bands detected at 849 cm^{-1} provided evidence for the existence of α-configuration sugar units in SRP-W-2[32]. The absence of distinctive absorption peaks associated with glucuronic acid and protein groups suggested that SRP-W-2 was a neutral sugar, aligning perfectly with the findings derived from monosaccharide composition analysis.

2.1.5 HPLC analysis

The monosaccharide composition of SRP-W-2 was analyzed using PMP precolumn derivatization (Figure 2C). A mixture of ten monosaccharide standards was separated and detected within a 35-minute timeframe. The monosaccharide compositions of SRP-W-2 were obtained under the same analytical conditions as the previous run. The results revealed that SRP-W-2 consisted predominantly of glucose and galactose, with a molar ratio of 12.53:1, respectively.

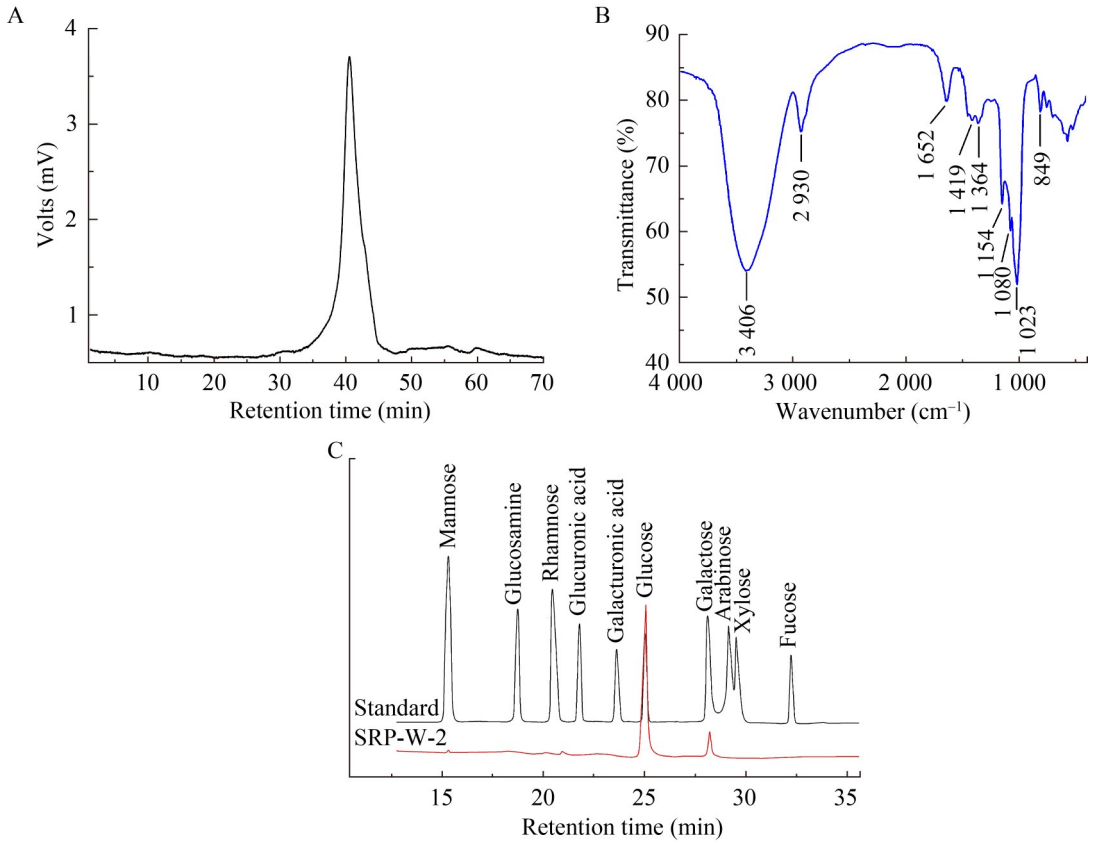

Figure 2 Structural characterization of SRP-W-2. A: HPGPC spectra; B: FT-IR spectra; C: Monosaccharide compositions.

2.1.6 GC-MS analysis

The glycosyl linkage types of SRP-W-2 were analyzed using GC-MS following acid hydrolysis, reduction, and acetylation[33]. The results of GC-MS spectra are summarized in Table 2. The SRP-W-2 sample exhibited the presence of four monosaccharide residues. Among these residues, 2, 3,6-tri-*O*-methyl glucitol constituted 56.37% of the total residues, suggesting that the primary chain of SRP-W-2 was composed of 1, 4-linked glucose units. Moreover, the presence of branched chains in SRP-W-2 was suggested by the proportion (16.52%) of 2,3-di-*O*-methyl glucitol. Additionally, 19.38% and 7.73% were attributed to 2, 3, 6-tri-*O*-methyl galactitol and 2, 3, 4, 6-tetra-*O*-methyl glucitol respectively, implying that both 1, 4-Gal*p* (galactose) and T-Glc*p* residues existed within the chains of SRP-W-2.

2.1.7 NMR spectrum analysis

To elucidate the connectivity sequence of sugar residues in SRP-W-2, we conducted 1D and 2D NMR spectroscopy analyses. The NMR spectra of SRP-W-2 were presented in Figure 3, while the chemical shift assignments can be found in Table 3. The main region of the SRP-W-2 hydrogen spectrum signal, as depicted in Figure 3A, was observed within the δ 3.00−5.50 ppm range, which was characteristic of saccharides. The anomeric signal region (δ 4.30−5.40 ppm) exhibited multiple coupling peaks, indicating the presence of sugar residues corresponding to chemical shifts of anomeric hydrogen at δ 5.28, 5.22, 5.18, 5.08 and 5.01 ppm for SRP-W-2 sample analyzed herein. The signals within the δ 3.0−4.3 ppm region of the hydrogen spectra represented typical signals outside the anomeric hydrogen range, however, due to significant overlap and numerous individual signals in this region, it was necessary to combine COSY and HSQC spectra for accurate assignment of H2-H6 chemical shifts for each sugar residue.

No carbonyl carbon signals corresponding to uronic acid were detected in the δ 160−180 region of the ^{13}C NMR spectra of SRP-W-2 (Figure 3B), confirming its neutral saccharide nature, consistent with its monosaccharide composition and FT-IR results. Furthermore, multiple signal peaks were observed in the anomeric carbon region for SPS2-A. By combining the cross peaks from the HSQC spectra (Figure 3D), the anomeric signals in SPS2-A were identified as δ 5.28/101.25, 5.22/100.89, 5.18/100.89, 5.08/99.43, and 5.01/99.38 ppm, indicating predominantly α-type glycosidic linkages composed of five monosaccharide residues designated as A, B, B′, C and D based on their respective chemical shift signal intensities[34].

According to the chemical shift δ 5.28/101.25 ppm of the anomeric signal H1/C1, as determined from the ^{1}H-^{1}H COSY spectrum (Figure 3C), the H_2 resonance (3.86 ppm) of residue A was assigned based on the cross peak at δ 5.28/3.86 ppm. Similarly, H3 (3.88 ppm), H4 (3.75 ppm) H5 (3.88 ppm), H6 (3.64, 3.75 ppm) of residue A were identified using cross peaks at δ 3.86/4.07, 4.07/3.57, 3.57/3.72 3.72/3.64, 3.75 ppm, respectively. Subsequently, carbon chemical shifts of residue A were assigned follows: C1 at δ 101.25, C2 at δ 72.52, C3 at δ 74.05, C4 at δ 78.03, C5 at δ 72.51, and C6 at δ 62.55 ppm using the HSQC spectrum (Figure 3D). The observed downfield chemical shift for positions C1 and C4 strongly indicated the

Table 2 Glycosidic linkages in SRP-W-2

Peak	Methylation products	Linkage type	Retention time (min)	Molar ratio	Molar ratio mass fragments (*m/z*)
1	2,3,4,6-Me_4-Glc	T-Glc*p*	13.56	19.38	43, 71, 87, 99, 102, 113, 118, 129, 145, 162, 205
2	2,3,6-Me_3-Gal	1,4-Gal*p*	16.41	7.73	43, 71, 87, 102, 113,118, 129, 142, 157, 162, 173, 233
3	2,3,6-Me_3-Glc	1,4-Glc*p*	16.73	56.37	43, 71, 87, 99, 102, 113, 118, 129, 142, 162, 173, 233
4	2,3-Me_2-Glc	1,4,6-Glc*p*	20.85	16.52	43, 71, 85, 99, 102, 118, 127, 142, 159, 201, 261

Me: Methyll; Glc*p*: Glucopyranose; Gal*p*: Galactopyranose.

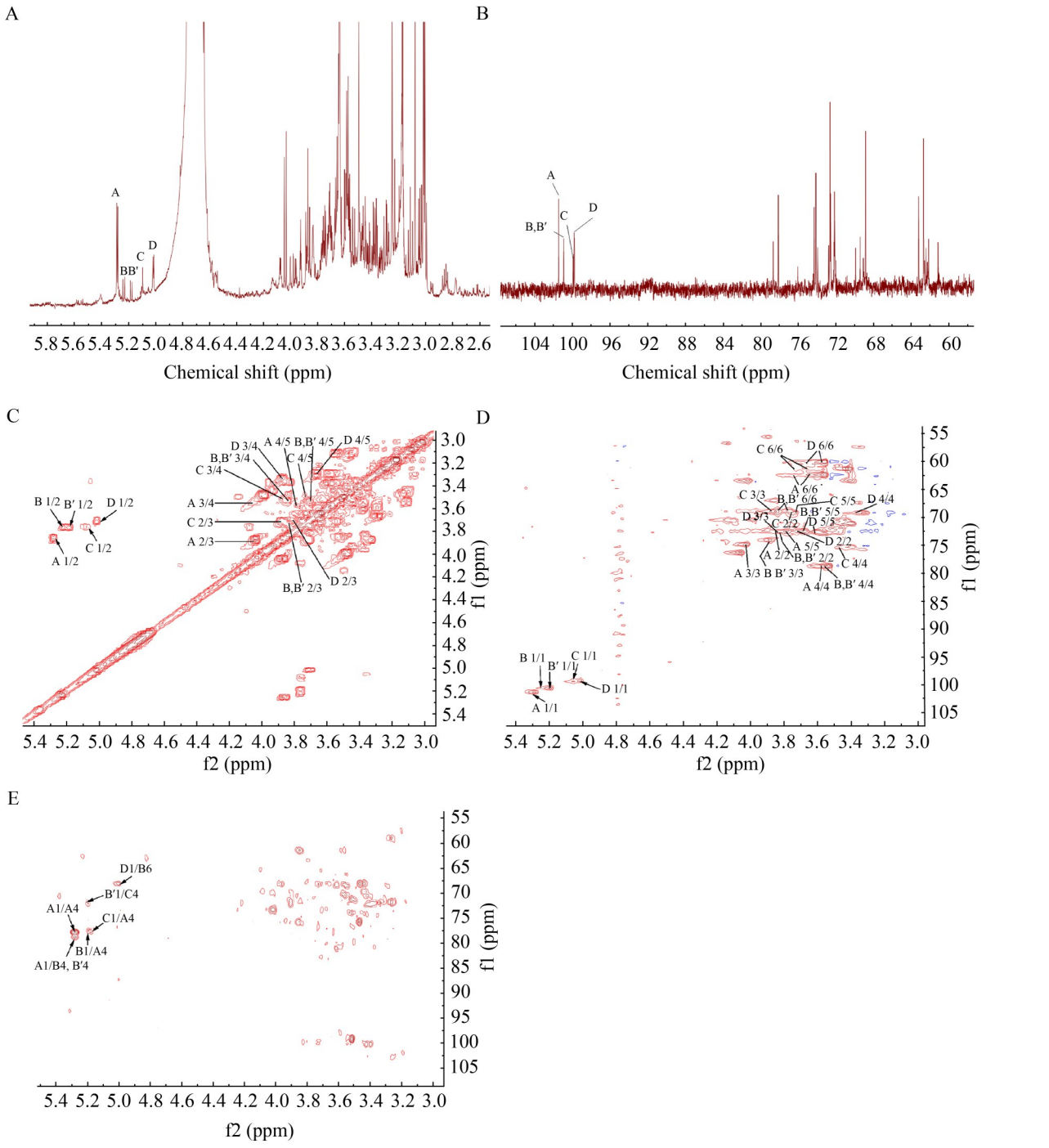

Figure 3 NMR spectra of SRP-W-2. A: 1H; B: 13C; C: 1H−1H COSY; D: HSQC; E: HMBC; F: The possible structure diagram of SRP-W-2. The interpretation of residues: A, →4)-α-D-Glc*p*-(1→; B and B′, →4,6)-α-D-Glc*p*-(1→; →4,6)-α-D-Glc*p*-(1→; C, →4)-α-D-Gal*p*-(1→; D, α-D-Glc*p*-(1→.

Table 3 ^{1}H and ^{13}C NMR chemical shift for SRP-W-2

Code	Glycosyl residues	Chemical shifts, δ (ppm)					
		H1/C1	H2/C2	H3/C3	H4/C4	H5/C5	H6a, b/C6
A	→4)-α-D-Glc*p*-(1→	5.28/101.25	3.86/72.52	4.07/74.05	3.57/78.03	3.72/72.51	3.64, 3.75/62.55
B	→4,6)-α-D-Glc*p*-(1→	5.22/100.89	3.77/72.49	3.83/73.90	3.54/78.25	3.70/72.18	3.75, 3.88/68.77
B'	→4,6)-α-D-Glc*p*-(1→	5.18/100.89	3.77/72.49	3.83/73.90	3.54/78.25	3.70/72.18	3.75, 3.88/68.77
C	→4)-α-D-Gal*p*-(1→	5.08/99.43	3.75/68.86	3.88/69.05	3.49/75.86	3.74/69.68	3.65, 3.74/62.18
D	T-α-D-Glc*p*	5.01/99.38	3.72/72.46	3.81/72.68	3.34/69.24	3.67/72.04	3.58, 3.70/61.09

replacement of residue A at positions O1 and O4 in the sugar ring. Based on these findings, residue A was designated as a →4)-α-D-Glc*p*-(1→. The other four residues were identified as →4,6)-α-D-Glc*p*-(1→(B, B′), →4)-α-D-Gal*p*-(1→ (C), and T-α-D-Glc*p* (D), respectively[35], using a similar methodology outlined in Table 2.

To further infer the interconnection between sugar residues, the HMBC spectrum was performed. The HMBC spectra of SRP-W-2 (Figure 3E) revealed the following coupling signals: H1 of residue A and C4 of residue A (A1/A4), H1 of residue A and C4 of residue B (A1/B4), H1 of residue A and C4 of residue B′ (A1/B′4), H1 of residue B and C4 of residue A (B1/A4), H1 of residue C and C4 of residue A (C1/A4), H1 of residue B′ and C4 of residue C (B′1/C4), H1 of residue D and C6 of residue B (D1/B6), respectively. Considering the molecular weight, monosaccharide, methylation, FT-IR, and 1D and 2D NMR characterization of SRP-W-2, the structure of SRP-W-2 was proposed and depicted in Figure 3F. The main chain of SRP-W-2 contained →4)-α-D-Glc*p*-(1→, →4)-α-D-Glc*p*-(1→ and →4)-α-D-Gal*p*-(1→. The branched chain consisted of α-D-Glc*p*-(1→4)-α-D-Glc*p*-(1→ connected to the O6 position of both residues →4,6)-α-D-Glc*p*-(1→ and →4,6)-α-D-Gal*p*-(1→.

2.2 Effects of SRP-W-2 on the growth, tanshinone accumulation, and gene expression in *S. miltiorrhiza* hairy roots

2.2.1 Effects of SRP-W-2 on biomass and tanshinone accumulation in the *S. miltiorrhiza* hairy roots

The influence of SRP-W-2 on the biomass of *S. miltiorrhiza* hairy roots was evaluated at 0, 5, 10, and 15 days, respectively. As shown in Figure 4A, the biomass of hairy roots exhibited a consistent increase during the cultivation period of 15 days. Notably, treatment groups with concentrations of SRP-W-2 at 25 mg/L and 50 mg/L demonstrated significant enhancements in root dry weight. Following a treatment duration of 10 days, the dry weight of hairy roots treated with SRP-W-2 at concentrations of both 25 mg/L and 50 mg/L showed a remarkable increase by 23.98% and 45.80%, respectively, compared to the control group. Similarly, after a treatment duration of 15 days, there was a significant increase in dry weight for hairy roots by 27.63% and 37.52%, respectively. Likewise, the polysaccharides tested in parallel (GLP) also exhibited significant promoting effects, which were comparable to those of SRP-W-2. The potential explanation lies in the fact that, on one hand, polysaccharides can enhance nutrient and mineral utilization efficiency in plants, while on the other hand, they exhibit hormone-like properties that stimulate plant growth[36]. However, the high concentration of SRP-W-2 (100 mg/L) did not significantly enhance hairy roots biomass throughout the coculture period compared to the control. These findings suggested the growth of hairy roots is more favorable under medium concentration of SRP-W-2 (50 mg/L) rather than high concentration of SRP-W-2 (100 mg/L), which aligned with a common phenomenon observed in other polysaccharide activators. For instance, the highest biomass accumulation of *Atractylodes macrocephala* Koidz was observed with a treatment of 2 mg/mL polysaccharide from *Chrysanthemum indicum* L. (CIP), while

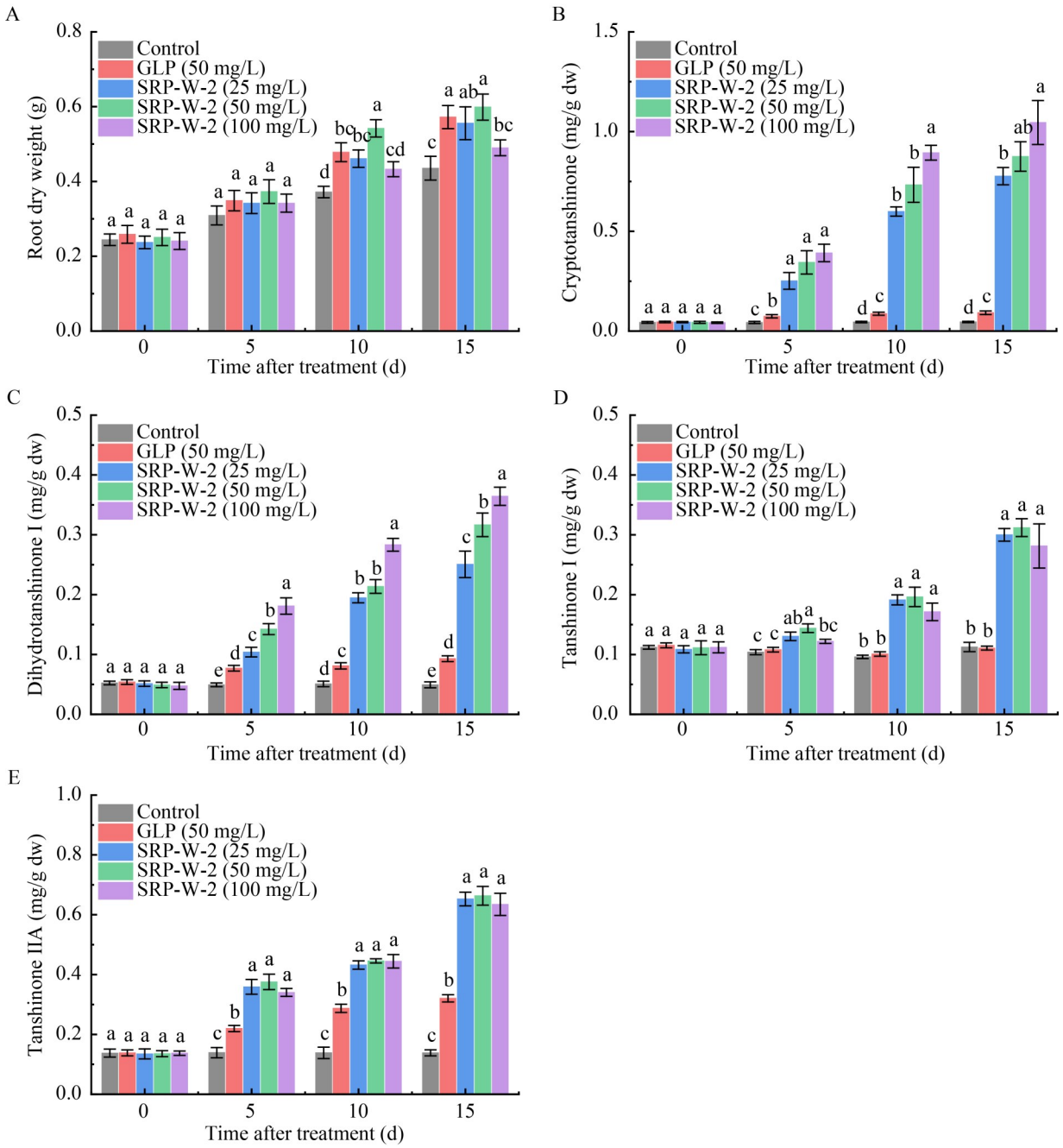

Figure 4 Effects of SRP-W-2 on biomass and tanshinone accumulation in the *Salvia miltiorrhiza* hairy roots. A: Root dry weight (dw); B: Cryptotanshinone; C: Dihydrotanshinone I; D: Tanshinone I; E: Tanshinone IIA. The values are presented as mean±SD (n=3). The use of different letters indicates statistical significance at P<0.05.

production decreased when treated with 10 mg/mL CIP[37]. It is postulated that lower concentrations of elicitors induce the upregulation of genes involved in biomass biosynthesis, leading to an increase in biomass[38]. However, excessive activation of these genes has deleterious effects on culture and results in reduced biomass yield[39]. The precise underlying mechanism necessitates further comprehensive investigation. Additionally, the presence of SRP-W-2 resulted in a more

pronounced red hue observed in both the color of hairy roots and their culture liquids after 15 days of cultivation. These variations in color are likely attributed to changes in the accumulation of tanshinones within the root periderm[40].

To further investigate the impact of SRP-W-2 on tanshinone biosynthesis in *S. miltiorrhiza* hairy roots, three concentrations of polysaccharide solutions were administered to induce stimulation in hairy roots. Subsequently, the levels of cryptotanshinone (CT), dihydrotanshinone I (DT-I), tanshinone I (T-I), and tanshinone IIA (T-IIA) were analyzed using a gradient elution protocol with HPLC. As shown in Figure 4B−4C, the treatment of SRP-W-2 resulted in a considerable alteration in the accumulation of the four tanshinones in hairy roots. Following a 5-day treatment, the levels of CT, DT-I, and T-IIA in hairy roots were significantly higher in all tested doses of SRP-W-2 compared with the blank and parallel controls. Meanwhile, SRP-W-2 significantly enhanced the synthesis of four tanshinones after 10 and 15 days of processing, particularly following a 15-day duration. The CT contents under the treatment of 25, 50, and 100 mg/L SRP-W-2 for 15 days exhibited a significant increase by up to 16.9, 19.0, and 22.7-fold that of the control, respectively (0.776, 0.875, and 1.045 *vs*. 0.046 mg/g dw, Figure 4B). Meanwhile, the T-I contents were significantly higher by a factor of approximately 2.7, 2.8, and 2.5-fold compared to the control (0.303, 0.312, and 0.281 *vs*. 0.113 mg/g dw, Figure 4C). Additionally, the DT-I contents showed a substantial increase by as much as 5.1, 6.4, and 7.4-fold that of the control (0.251, 0.317, and 0.364 *vs*. 0.049 mg/g dw, Figure 4D), while the T-IIA contents demonstrated an elevation by as much as 4.7, 4.8, and 4.9-fold that of the control (0.653, 0.663, and 0.672 *vs*. 0.138 mg/g dw, Figure 4E). Upon comparison with the parallel control group and extant literature, it becomes manifest that SRP-W-2 exerted a more potent stimulatory effect on the biosynthesis of tanshinone in *S. miltiorrhiza* hairy roots than numerous contemporary inducers, including biotic elicitors and abiotic elicitors[19]. Our findings indicate that SRP-W-2 effectively enhances tanshinone biosynthesis in hairy root cultures. Although the parallel control group (GLP) also exhibited a significant increase in the contents of CT, DT-I, and T-IIA compared to the blank control, these levels remained considerably lower than those observed with SRP-W-2 treatment. As is well-established, the bioactivity of polysaccharides is closely associated with their composition and structural features. We thus hypothesize that the α-configuration and the O-6 branch of SRP-W-2 may contribute to its biological activity—a premise that warrants further experimental validation. Moreover, it is emphasized that future studies should focus on identifying the active domain of SRP-W-2 to elucidate its regulatory mechanism in greater detail.

2.2.2 Effects of SRP-W-2 on the expressions of genes HMGR, DXS, DXR, and GGPPS in *S. miltiorrhiza* hairy roots

The biosynthesis pathway of tanshinones involves both the mevalonate (MVA) and methylerythritol phosphate (MEP) pathways[41]. Key enzymes involved in tanshinone biosynthesis include *HMGR* genes in the MVA pathway, *DXS* and *DXR* genes in the MEP pathway, and *GGPPS* genes in the downstream pathway[42]. To further elucidate the mechanism behind SRP-W-2-induced accumulation of tanshinone in hairy roots, we selected four key genes involved in tanshinone biosynthesis (*HMGR*, *DXS*, *DXR*, and *GGPPS*) and assessed their relative expression levels under control conditions and treatment with 50 mg/L of SRP-W-2. The treatment of SRP-W-2 (50 mg/L) significantly impacted the gene expressions of four key enzymes in *S. miltiorrhiza* hairy roots, as illustrated in Figure 5. The observed trend indicates an initial increase followed by a subsequent decrease. The expression levels of the genes *HMGR* and *GGPPS* were significantly upregulated by 12.0-fold and 17.7-fold, respectively, compared to the control after a 10-day treatment (Figure 5A−5D). Furthermore, following a 5-day treatment, the

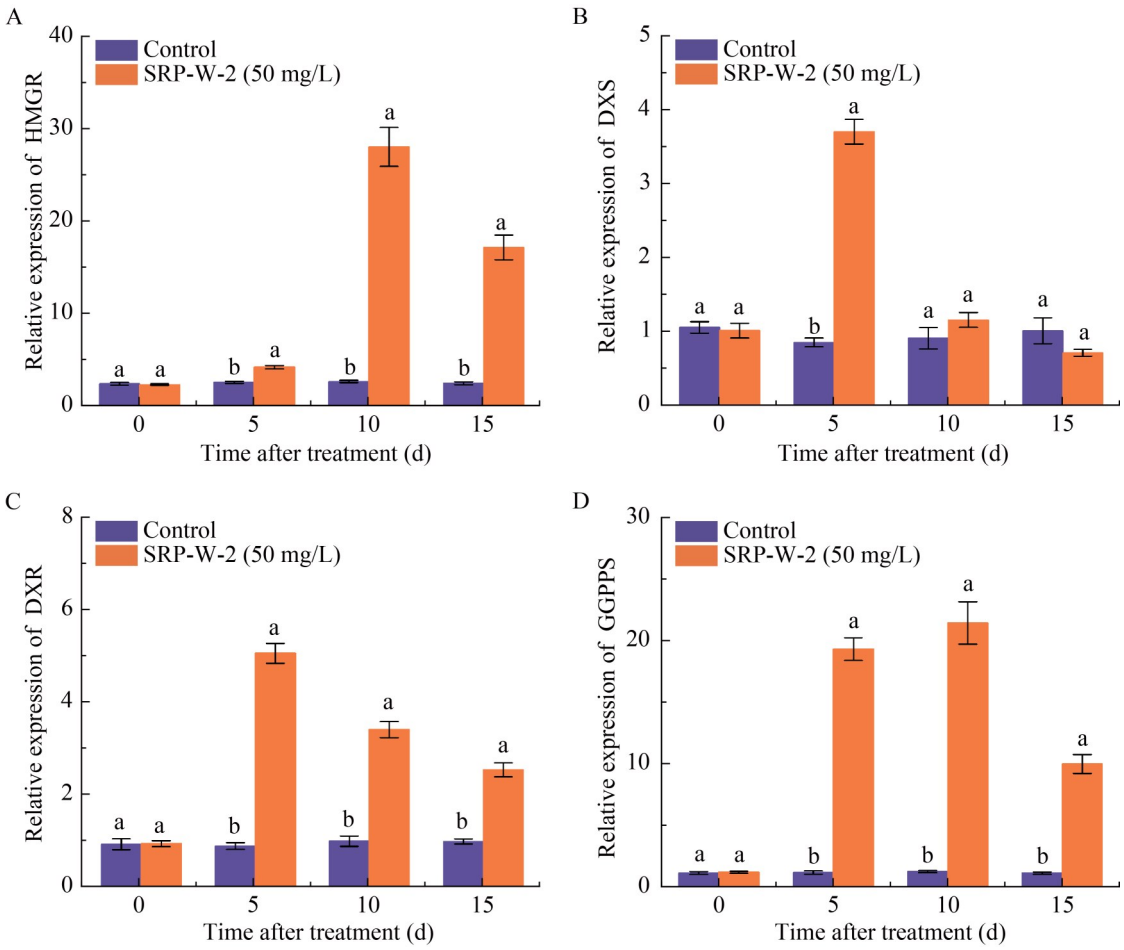

Figure 5 Effects of SRP-W-2 on the expression of the four key enzymes in *Salvia miltiorrhiza* hairy roots. A: 3-hydroxy-3-methylglutary coenzyme A reductase (*HMGR*); B: 1-deoxy-D-xylulose-5-phosphate synthase (*DXS*); C: 1-deoxy-D-xylulose-5-phosphate reductoisomerase (*DXR*); D: Geranylgeranyl diphosphate synthase (*GGPPS*). The data are presented as mean±SD (n=3), with different letters indicating statistical significance at P<0.05.

expressions of *DXS* and *DXR* genes were significantly increased by approximately 3.7-fold and 5.4-fold higher than that of the control, respectively (Figure 5B−5C). The observed results were consistent with the accumulation of tanshinone induced by SRP-W-2, indicating that the synthesis of tanshinone in *S. miltiorrhiza* hairy roots primarily relied on both the MVA and MEP pathways facilitated by SRP-W-2. This highlights the ability of SRP-W-2 to efficiently modulate secondary metabolism at the genetic level. However, due to the diversity and complexity of tanshinone metabolic pathways, the precise routes have not been fully elucidated. Furthermore, obtaining a high-quality genome would be an optimal approach for unraveling the mechanisms underlying tanshinone synthesis in *S. miltiorrhiza* hairy roots. Consequently, we intend to conduct an extensive investigation on SRP-W-2-induced transcriptome data in future studies.

3 Conclusion

In this work, a polysaccharide (SRP-W-2) was isolated from *Streptomyces rochei* D74 with a molecular weight of 44.7 kDa and composed of glucose and galactose, in a molar ratio of 12.53∶1,

respectively. The SRP-W-2 domains were mainly composed of →4)-α-D-Glc*p*-(1→, →4,6)-α-D-Glc*p*-(1→, →4)-α-D-Gal*p*-(1→, and T-α-D-Glc*p*. The bioactivity tests demonstrated that SRP-W-2 significantly enhanced biomass accumulation and stimulated the biosynthesis of CT, DT-I, T-I, and T-IIA in *S. miltiorrhiza* hairy roots. Subsequent investigations revealed that SRP-W-2 upregulated the expression of key biosynthetic genes (*HMGR*, *DXS*, *DXR*, and *GGPPS*) at the transcript level in *S. miltiorrhiza* hairy roots, leading to improved tanshinones accumulation. These findings of this study suggest that SRP-W-2 exhibits significant potential as a potent stimulator for augmenting biomass and tanshinone yield in *S. miltiorrhiza* hairy roots production.

Credit authorship contribution statement

MA Fang: Writing-original draft, visualization, software, methodology, formal analysis, data curation, conceptualization; ZHANG Bingying: Writing-original draft, methodology, formal analysis, data curation; LI Yang: methodology, formal analysis, resources, data curation; WANG Siyu: Methodology, formal analysis, data curation; XUE Quanhong: Visualization, resources; DU Hongtao: Writing-review & editing, supervision, resources, funding acquisition, conceptualization; YAN Yan: Funding acquisition, investigation, resources.

Declaration of competing interest

The authors declare no competing financial interest.

References

[1] 国家药典委员会. 中华人民共和国药典-一部2020年版[M]. 北京: 中国医药科技出版社, 2020: 77-79.
Chinese Pharmacopoeia Commission. Pharmacopoeia of the People's Republic of China: Voloum 1[M]. Beijing: China Medical Science Press, 2020: 77-79 (in Chinese).

[2] XU ZC, JI AJ, ZHANG X, SONG JY, CHEN SL. Biosynthesis and regulation of active compounds in medicinal model plant *Salvia miltiorrhiza*[J]. Chinese Herbal Medicines, 2016, 8(1): 3-11.

[3] 李桃桃, 洪阁, 刘玥彤, 刘天军. 丹参酮抗肿瘤作用的研究进展[J]. 现代药物与临床, 2024, 39(12): 3246-3253.
LI TT, HONG G, LIU YT, LIU TJ. Research progress on anti-tumor effect of tanshinones[J]. Drugs & Clinic, 2024, 39(12): 3246-3253 (in Chinese).

[4] YANG Y, SHAO MY, CHENG WK, YAO JK, MA L, WANG Y, WANG W. A pharmacological review of tanshinones, naturally occurring monomers from *Salvia miltiorrhiza* for the treatment of cardiovascular diseases[J]. Oxidative Medicine and Cellular Longevity, 2023, 2023: 3801908.

[5] RASTEGARNEJAD F, MIRJALILI MH, BAKHTIAR Z. Enhanced production of tanshinone and phenolic compounds in hairy roots culture of *Salvia miltiorrhiza* Bunge by elicitation[J]. Plant Cell, Tissue and Organ Culture (PCTOC), 2023, 156(1): 4.

[6] 包丽琼, 陈同, 靳保龙, 李奉胜, 李佐君, 陈美兰, 王铁霖, 崔光红, 黄璐琦. 丹参酮类化合物调控丹参根微生物组的研究[J]. 中国中药杂志, 2021, 46(11): 2806-2815.
BAO LQ, CHEN T, JIN BL, LI FS, LI ZJ, CHEN ML, WANG TL, CUI GH, HUANG LQ. Study on tanshinones regulating root-associated microbiomes of *Salvia miltiorrhiza*[J]. China Journal of Chinese Materia Medica, 2021, 46(11): 2806-2815 (in Chinese).

[7] 李俊伶, 吴家慧, 李堰, 李侯希尔, 张大川, 谭淑渟, 王楠, 王学勇. 复合诱导子不同处理时间对丹参毛状根生长和初次生代谢产物积累的影响[J]. 中南药学, 2023, 21(6): 1422-1428.
LI JL, WU JH, LI Y, LI HXE, ZHANG DC, TAN ST, WANG N, WANG XY. Effect of different treatment time of combined elicitors on the growth of *Salvia miltiorrhiza* hairy roots and accumulation of the primary and secondary metabolites[J]. Central South Pharmacy, 2023, 21(6): 1422-1428 (in Chinese).

[8] WU SJ, XIE XG, FENG KM, ZHAI X, MING QL, QIN LP, RAHMAN K, ZHANG ZZ, HAN T. Transcriptome sequencing and signal transduction for the enhanced tanshinone production in *Salvia miltiorrhiza* hairy roots induced by *Trichoderma atroviride* D16 polysaccharide fraction[J]. Bioscience, Biotechnology, and Biochemistry, 2022, 86(8): 1049-1059.

[9] LI J, LI CL, DENG YX, WEI HR, LU SF. Characteristics of *Salvia miltiorrhiza* methylome and the regulatory mechanism of DNA methylation in tanshinone biosynthesis[J]. Horticulture Research, 2023, 10(7): uhad114.

[10] LU WL, XIE XG, AI HW, WU HF, DAI YY, WANG LN, RAHMAN K, SU J, SUN K, HAN T. Crosstalk between H_2O_2 and Ca^{2+} signaling is involved in root endophyte-enhanced tanshinone biosynthesis of *Salvia miltiorrhiza*[J]. Microbiological Research, 2024, 285: 127740.

[11] BAGAL D, ALI CHOWDHARY A, MEHROTRA S, MISHRA S, RATHORE S, SRIVASTAVA V. Metabolic engineering in hairy roots: an outlook on production of plant secondary metabolites[J]. Plant Physiology and Biochemistry, 2023, 201: 107847.

[12] KHALILI HASSANABAD M, MIRJALILI MH, MOHAJERI M. Boosted centellosides production in

Gotu kola (*Centella asiatica*) transgenic hairy roots elicited by gold and zinc nanoparticles[J]. Industrial Crops and Products, 2025, 227: 120796.
[13] ZHANG B, HUO YB, ZHANG J, ZHANG X, ZHU CS. *Agrobacterium rhizogenes*-mediated RNAi of *Tripterygium wilfordii* and application for functional study of terpenoid biosynthesis pathway genes[J]. Industrial Crops and Products, 2019, 139: 111509.
[14] HASEBE F, YUBA H, HASHIMOTO T, SAITO K, FUNA N, SHOJI T. Crispr/Cas9-mediated disruption of the pyrrolidine ketide synthase gene reduces the accumulation of tropane alkaloids in *Atropa belladonna* hairy roots[J]. Bioscience, Biotechnology, and Biochemistry, 2021, 85(12): 2404-2409.
[15] LI JW, ZENG T, XU ZZ, LI JJ, HU H, YU Q, ZHOU L, ZHENG RR, LUO J, WANG CY. Ribozyme-mediated CRISPR/Cas9 gene editing in *Pyrethrum* (*Tanacetum cinerariifolium*) hairy roots using a RNA polymerase II-dependent promoter[J]. Plant Methods, 2022, 18(1): 32.
[16] LI CL, WANG MZ. Application of hairy root culture for bioactive compounds production in medicinal plants[J]. Current Pharmaceutical Biotechnology, 2021, 22(5): 592-608.
[17] MMEREKE KM, VENKATARAMAN S, MOIKETSI BN, KHAN MR, HASSAN SH, RANTONG G, MASISI K, KWAPE TE, GAOBOTSE G, ZULFIQAR F, KUMAR SHARMA S, MALIK S, MAKHZOUM A. Nanoparticle elicitation: a promising strategy to modulate the production of bioactive compounds in hairy roots[J]. Food Research International, 2024, 178: 113910.
[18] 王飞艳, 尤华乾, 杜旭红, 杨宗岐, 张晓丹, 梁宗锁, 杨东风. 不同氮源对丹参和藏丹参毛状根有效成分积累的影响[J]. 中草药, 2020, 51(9): 2538-2547.
WANG FY, YOU HQ, DU XH, YANG ZQ, ZHANG XD, LIANG ZS, YANG DF. Effects of different nitrogen sources on accumulation of active components in hairy roots of *Salvia miltiorrhiza* and *Salvia castanea* f. tomentosa[J]. Chinese Traditional and Herbal Drugs, 2020, 51(9): 2538-2547 (in Chinese).
[19] WU JJ, MING QL, ZHAI X, WANG SQ, ZHU B, ZHANG QL, XU YB, SHI SS, WANG SC, ZHANG QY, HAN T, QIN LP. Structure of a polysaccharide from *Trichoderma atroviride* and its promotion on tanshinones production in *Salvia miltiorrhiza* hairy roots[J]. Carbohydrate Polymers, 2019, 223: 115125.
[20] YANG BC, LEE MS, LIN MK, CHANG WT. 5-azacytidine increases tanshinone production in *Salvia miltiorrhiza* hairy roots through epigenetic modulation[J]. Scientific Reports, 2022, 12: 9349.
[21] WANG YM, CAI SY, TAO ZL, PENG JZ, LI D, LI LD, CAO XY, JIANG JH. Isolation of endophytic fungi and effects on secondary metabolites in hairy roots of *Salvia miltiorrhiza*[J]. Journal of Microbiology and Biotechnology, 2025, 35: e2411051.
[22] XI J, DING ZB, XU TQ, QU WX, XU YZ, MA YQ, XUE QH, LIU YX, LIN YB. Maize rotation combined with *Streptomyces rochei* D74 to eliminate orobanche cumana seed bank in the farmland[J]. Agronomy, 2022, 12(12): 3129.
[23] 席娇, 徐腾起, 刘玉涛, 马永清, 薛泉宏, 林雁冰. *Streptomyces rochei* D74菌剂对向日葵、列当及其根际微生物的影响[J]. 微生物学报, 2023, 63(2): 745-759.
XI J, XU TQ, LIU YT, MA YQ, XUE QH, LIN YB. Effect of *Streptomyces rochei* D74 on sunflower, *Orobanche cumana*, and their rhizosphere microorganisms[J]. Acta Microbiologica Sinica, 2023, 63(2): 745-759 (in Chinese).
[24] QIAO MX, LV SY, QIAO YJ, LIN W, GAO ZQ, TANG XW, YANG ZP, CHEN J. Exogenous *Streptomyces* spp. enhance the drought resistance of naked oat (*Avena nuda*) seedlings by augmenting both the osmoregulation mechanisms and antioxidant capacities[J]. Functional Plant Biology, 2024, 51: FP23312.
[25] DUBOIS M, GILLES KA, HAMILTON JK, REBERS PA, SMITH F. Colorimetric method for determination of sugars and related substances[J]. Analytical Chemistry, 1956, 28(3): 350-356.
[26] BITTER T, MUIR HM. A modified uronic acid carbazole reaction[J]. Analytical Biochemistry, 1962, 4(4): 330-334.
[27] BRADFORD MM. A rapid and sensitive method for the quantitation of microgram quantities of protein utilizing the principle of protein-dye binding[J]. Analytical Biochemistry, 1976, 72(1/2): 248-254.
[28] DU HT, CHEN JC, TIAN S, GU HL, LI N, SUN Y, RU JJ, WANG JR. Extraction optimization, preliminary characterization and immunological activities *in vitro* of polysaccharides from *Elaeagnus angustifolia* L. pulp[J]. Carbohydrate Polymers, 2016, 151: 348-357.
[29] WANG YL, HAN J, YUE Y, WU YZ, ZHANG WQ, XIA W, WU MQ. Purification, structure identification and immune activity of a neutral polysaccharide from *Cynanchum auriculatum*[J]. International Journal of Biological Macromolecules, 2023, 237: 124142.
[30] CHEN HM, CHEN JL, QI Y, CHU SY, MA Y, XU LN, LV SY, ZHANG HH, YANG DF, ZHU YH, MANS DR, LIANG ZS. Endophytic fungus *Cladosporium tenuissimum* DF11, an efficient inducer of tanshinone biosynthesis in *Salvia miltiorrhiza* roots[J]. Phytochemistry, 2022, 194: 113021.
[31] FENG L, SHI PX, ZHAO LC, SHANG MW, HAN YB, HAN N, LIU ZH, LI SK, ZHAI JX, YIN J. Structural characterization of polysaccharides from *Panax ginseng* C. A. Meyer root and their triggered potential immunoregulatory and radioprotective activities[J]. International Journal of Biological Macromolecules, 2024, 280(Pt 3): 135993.
[32] WANG XP, ZHAO CY, WANG JR, LU XM, BAO YM, ZHANG DL, ZHENG JK. Structure characterization and gelling properties of RG-I-enriched pectins extracted from citrus peels using four different methods[J]. Carbohydrate Polymers, 2024, 342: 122410.
[33] HUANG JW, WANG HQ, CHEN HQ, LIU ZD, ZHANG XD, TANG H, WEI SY, ZHOU WT, YANG XZ, LIU YH, ZHAO LY, YUAN QX. Structural analysis and *in vitro* fermentation characteristics of an *Avicennia marina* fruit RG-I pectin as a potential prebiotic[J]. Carbohydrate Polymers, 2024, 338: 122236.

[34] PEI WH, LI M, WU JH, HUANG MQ, SUN BG, LIANG HY, WU ZY. Preparation, structural analysis, and intestinal probiotic properties of a novel oligosaccharide from enzymatic degradation of Huangshui polysaccharide[J]. Journal of Agricultural and Food Chemistry, 2024, 72(1): 313-325.
[35] CAI Y, SI ZY, JIANG Y, YE M, WANG F, YANG XB, YU JP, GAO XD, LIU W. Structure-activity relationship of low molecular weight *Astragalus membranaceus* polysaccharides produced by *Bacteroides*[J]. Carbohydrate Polymers, 2023, 316: 121036.
[36] HERNÁNDEZ-HERRERA RM, SANTACRUZ-RUVALCABA F, ZAÑUDO-HERNÁNDEZ J, HERNÁNDEZ-CARMONA G. Activity of seaweed extracts and polysaccharide-enriched extracts from *Ulva lactuca* and *Padina gymnospora* as growth promoters of tomato and mung bean plants[J]. Journal of Applied Phycology, 2016, 28(4): 2549-2560.
[37] ZHOU YL, LU XF, CHEN L, ZHANG PF, ZHOU JQ, XIONG QW, SHEN YR, TIAN W. Polysaccharides from *Chrysanthemun indicum* L. enhance the accumulation of polysaccharide and atractylenolide in *Atractylodes macrocephala* Koidz[J]. International Journal of Biological Macromolecules, 2021, 190: 649-659.
[38] AWAD V, KUVALEKAR A, HARSULKAR A. Microbial elicitation in root cultures of *Taverniera cuneifolia* (Roth) Arn. for elevated glycyrrhizic acid production[J]. Industrial Crops and Products, 2014, 54: 13-16.
[39] SAKUNPHUEAK A, PANICHAYUPAKARANANT P. Increased production of naphthoquinones in *Impatiens balsamina* root cultures by elicitation with methyl jasmonate[J]. Bioresource Technology, 2010, 101(22): 8777-8783.
[40] THAKUR M, BHATTACHARYA S, KHOSLA PK, PURI S. Improving production of plant secondary metabolites through biotic and abiotic elicitation[J]. Journal of Applied Research on Medicinal and Aromatic Plants, 2019, 12: 1-12.
[41] ZHANG Y, HAO L, LIU XC, ZHANG FY, BAI XL, ZHANG YM. Alternative splicing of tanshinone synthesis genes and related splicing factors in *Salvia miltiorrhiza* in response to hormones[J]. Industrial Crops and Products, 2025, 224: 120372.
[42] YAN Y, ZHANG SC, YANG DF, ZHANG JY, LIANG ZS. Effects of *Streptomyces pactum* Act12 on *Salvia miltiorrhiza* hairy root growth and tanshinone synthesis and its mechanisms[J]. Applied Biochemistry and Biotechnology, 2014, 173(4): 883-893.